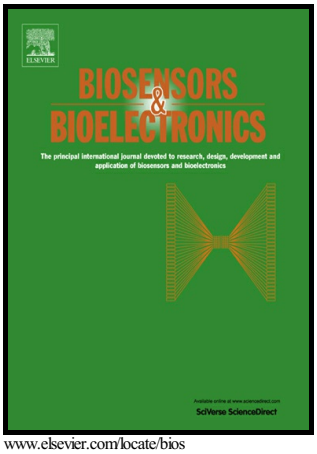

www.elsevier.com/locate/bios

Field-Effect Transistor Biosensors with Two-dimensional Black Phosphorus Nanosheets

Yantao Chen, Ren Ren, Haihui Pu, Jingbo Chang, Shun Mao, Junhong Chen

PII: S0956-5663(16)30251-2
DOI: http://dx.doi.org/10.1016/j.bios.2016.03.059
Reference: BIOS8570

To appear in: *Biosensors and Bioelectronic*

Received date: 31 December 2015
Revised date: 21 March 2016
Accepted date: 23 March 2016

Cite this article as: Yantao Chen, Ren Ren, Haihui Pu, Jingbo Chang, Shun Mac and Junhong Chen, Field-Effect Transistor Biosensors with Two-dimensiona Black Phosphorus Nanosheets, *Biosensors and Bioelectronic* http://dx.doi.org/10.1016/j.bios.2016.03.059

Field-Effect Transistor Biosensors with Two-dimensional Black Phosphorus Nanosheets

Yantao Chen [a], Ren Ren [a], Haihui Pu [a], Jingbo Chang [a], Shun Mao [a,b,], Junhong Chen [a,]**

[a] Department of Mechanical Engineering, University of Wisconsin-Milwaukee, 3200 N. Cramer Street, Milwaukee, WI 53211, USA

[b] State Key Laboratory of Pollution Control and Resource Reuse, School of Environmental Science and Engineering, Tongji University, 1239 Siping Road, Shanghai 200092, PR China

*Corresponding authors. E-mail addresses: jhchen@uwm.edu (J. Chen), shunmao@uwm.edu (S. Mao)

ABSTRACT:

A black phosphorous (BP)-based field-effect transistor (FET) biosensor was fabricated by using few-layer BP nanosheets labeled with gold nanoparticle-antibody conjugates. BP nanosheets were mechanically exfoliated and used as the sensing/conducting channel in the FET, with an Al_2O_3 thin film as the dielectric layer for surface passivation. Antibody probes were conjugated with gold nanoparticles that were sputtered on the BP through surface functionalization. The sensor response was measured by the change in the BP's electrical resistance after antigens were introduced. The adsorbed antigens through specific antigen-antibody binding interactions induced a gate potential, thereby changing the drain-source current. The as-produced BP biosensor showed both high sensitivity (lower limit of detection ~10 ng/ml) and selectivity towards human immunoglobulin G. Results from this study demonstrate the outstanding performance of BP as a sensing channel for FET biosensor applications.

KEYWORDS: Phosphorene nanosheet, Field-effect transistor, Biosensor, Protein detection, Immunoglobulin G

1. Introduction

Two-dimensional (2D) nanomaterials, such as graphene and metal dichalcogenides, have attracted increasing attention due to their unique structure and properties (Coleman et al. 2011), which stimulated the interdisciplinary research in physics, chemistry, biomedicine and electronics (Radisavljevic et al. 2011; Yang et al. 2010). Because graphene and metal dichalcogenide nanosheets are sensitive to electronic perturbations resulting from surface adsorption and modification (Schedin et al. 2007), those 2D materials have been widely studied for biosensors (Mao et al. 2013) (Mao et al. 2010; Sarkar et al. 2014), gas sensors (Schedin et al. 2007) (Li et al. 2012) (Late et al. 2013) and water sensors (Chen et al. 2012) (Chang et al. 2015). Black phosphorus (BP), the most stable allotrope in the phosphorus family with an orthorhombic lattice, is a recently rediscovered 2D layered crystal in which the monolayer (i.e., phosphorene) sheets stack together through van der Waals interactions with an interlayer spacing of 5.3 Å (Li et al. 2014) (Xia et al. 2014). Unlike the semi-metallic graphene or indirect band gap metal dichalcogenides, BP has a direct and thickness-dependent band gap that varies from 0.3 eV for the bulk BP to 2.0 eV for the monolayer BP (Dai and Zeng 2014; Li et al. 2014). Transfer characteristics of BP-based devices have shown the well-developed current saturation with a large on-off current ratio ($> 10^5$) (Li et al. 2014). Moreover, BP also exhibits a high carrier mobility and the field-effect extracted carrier mobility can reach up to ~1,000 $cm^2V^{-1}s^{-1}$ for a 10 nm-thick BP nanoflake at room temperature (Li et al. 2014), much larger than the carrier mobility (~200 $cm^2V^{-1}s^{-1}$) for MoS_2 (Radisavljevic and Kis 2013). Therefore, the wide band gap range and the high carrier mobility make BP an attractive material for various electronic/optoelectronic device applications.

Recently, the field-effect transistor of few-layer BP has attracted growing attention for high-performance sensor applications. Zhou *et al.* reported that BP nanosheets-based field-effect transistor (FET) gas sensors show superior sensing performance towards NO_2 with a lower detection limit down to 5 ppb (Abbas et al. 2015). Meanwhile, Cui *et al*. demonstrated that the BP-based sensor features an ultrahigh gas adsorption density and layer-dependent sensitivity (Cui et al. 2015). Importantly, the excellent sensing performance of BP is ascribed to its finite band gap and high carrier mobility (Cui et al. 2015), which could also be used for the detection of other types of adsorbates such as biomolecules. For example, Zhang *et al.* reported that BP has a unique interaction mechanism with proteins due to the puckered surface morphology (Zhang et al. 2015), which suggests BP's potential application for biosensors. In principle, to be used as the channel material in an FET sensor, thin BP flakes can be fabricated by either liquid or mechanical exfoliation of bulk BP (Brent et al. 2014; Li et al. 2014) to bridge the source and drain electrodes. However, the as-produced BP nanosheets are unstable under the ambient condition since significant surface roughening can occur within one hour of exposure to air (Wood et al. 2014) (Koenig et al. 2014). Wood *et al.* reported that O_2-saturated water can irreversibly react with BP to form oxidized phosphorous species, leading to an increased threshold voltage and degraded electronic properties (Wood et al. 2014). They further found that atomic layer deposition (ALD) of AlO_x can effectively passivate the surface of BP nanosheets and the measurements of the transfer characteristics showed that the high on/off current ratio and mobility could be maintained over two weeks under ambient conditions (Wood et al. 2014). There have been quite a few published works regarding the protein sensing application of novel semiconductor materials. For example, Li *et al.* reported that specific antibody functionalized carbon nanotubes can be used as the sensing channel to detect prostate-specific antigen (Li et al.

2005). Ohno *et al.* demonstrated that the immunoglobulin E (IgE) aptamers immobilized graphene FET sensor shows a real-time response to IgE molecules (Ohno et al. 2010). And a more recent study shows that biotin functionalized few-layer MoS_2 FET device can be used in detecting streptavidin with a higher sensitivity than graphene due to MoS_2's unique band gap (Sarkar et al. 2014). Discovering semiconductor materials with better electrical properties as the conducting channel can help to improve the overall performance of the FET biosensor. Our study shows the possibility of using surface-passivated BP as the sensing channel for the detection of biomolecules under aqueous conditions.

Here, we report using a mechanical exfoliation (Scotch tape) method (Li et al. 2014) to fabricate few-layer BP nanosheets for human immunoglobulin G (IgG) detection. The as-produced device was coated with an Al_2O_3 thin film for surface passivation by using ALD. Anti-human IgG-conjugated gold nanoparticles were deposited on the surface of Al_2O_3 dielectric layer as the probes for antigen (IgG) detection. After the IgG was pipetted onto the sensor, the binding of antibody and IgG induced a significant change in the BP's electrical conductivity, which was recorded as the sensing signal. The BP-based FET sensor shows good stability under the ambient condition for about one week with relatively small changes in the electrical resistance and on-off current ratio (Fig. S1). The sensor exhibits a high sensitivity (down to 10 ng/ml) to human IgG with a response time on the order of seconds. This study demonstrates the potential of using BP as the sensing channel in the FET biosensor for biomolecule detection. We believe this study will expand the 2D material applications in FET biosensors especially for beyond-graphene based nanomaterials.

2. Material and methods

2.1 Device fabrication

Gold interdigitated electrodes with inter-finger spacing of 1.5 μm and thickness of 50 nm were fabricated by using e-beam lithography on a highly doped silicon wafer with an SiO_2 top layer (thickness of 200 nm). BP nanosheets were mechanically exfoliated from commercial bulk BP by using a "Scotch tape" method (Buscema et al. 2014; Cui et al. 2015) and then transferred onto gold electrodes. The BP device was annealed in argon flow (1 L/min) at 250 °C for 30 minutes to improve the electrical contact between BP nanosheets and gold electrodes. A thin layer of Al_2O_3 (thickness ~ 3 nm) was grown on the surface of BP nanosheets by using ALD (CambridgeNanoTech, Savannah 100) for surface passivation. Gold nanoparticles (NPs) were deposited onto the surface of the BP device by using an RF (60 Hz) Emitech K550x sputter coater apparatus with a gold target. Gold NPs on the BP surface were functionalized with the cysteamine solution (1 mg/mL, Aldrich) for 30 minutes, followed by the glutaraldehyde solution (50% in water, Sigma) for one hour (Chang et al. 2013b). The anti-human IgG (Sigma) was pipetted onto the sensing area of the BP device to be conjugated with the functionalized gold NPs, and then the device was incubated at room temperature for one hour. Finally, the device was incubated in the blocking buffer (SuperBlock T20, Thermo Scientific) for another hour to avoid non-specific protein bindings to BP nanosheets. The BP device was thoroughly washed with DI water and dried with compressed air to remove the excess chemicals after each step of functionalization.

2.2 Structure characterization

A Hitachi S-4800 UHR FE-SEM was used for characterizing the BP device with an acceleration voltage of 10 kV. Raman spectroscopy was conducted using a Renishaw Raman

spectrometer (Inc 1000B) with a HeNe laser. Atomic force microscopy (AFM) was conducted using an Agilent Technology 5420 AFM with a cantilever (Nanosensors PPP-NCH).

2.3 Sensor performance characterization

A Keithley 4200 semiconductor characterization system was used for the sensor device electrical property characterization (direct current and transistor measurements) and sensing tests (dynamic measurements). The direct current measurement was performed by recording the drain current with the drain-source voltage V_{ds} sweeping from -2.0 to +2.0 V. In the transistor measurement, the drain current was measured with a fixed V_{ds} (0.01 V) while sweeping the gate voltage V_g from -40.0 to +40.0 V. The dynamic measurement was carried out by recording the drain current with a fixed V_{ds} (0.01 V). The sensing test was performed in an ambient environment at room temperature and the sensor repeatability was studied by using four sensors under each sensing test/condition.

3. Results and discussion

Fig. 1 shows a schematic of the BP FET device where antibody probes were immobilized on the BP nanosheet for specific binding to antigen. Scanning electron microscopy (SEM) was conducted on the BP sensor for investigating the structure of the as-produced device. As shown in the SEM image in Fig. 2A, transparent BP nanosheets bridge the gap between the finger electrodes, serving as the conducting channel. The typical size of the nanosheets varies from several hundred nanometers to several microns. Since the gap of the electrode is 1.5 μm, only nanosheets that can bridge the gap function in the sensor. As shown in the inset of Fig. 2A, isolated gold NPs with a size of ~5 nm were uniformly and densely distributed on the BP

nanosheet. The uniform and non-continuous distribution of gold NPs is critical for the sensor performance. A high density of gold NPs may lead to a high density of antibodies in the sensor, which could enhance the sensor response upon the antigen binding (Mao et al. 2011). However, if the NP density is too high, a continuous layer of NPs may form and thus short the sensor circuit. The 'Scotch tape' method could produce BP nanosheets with various thicknesses. AFM was used to characterize the exfoliated BP nanosheets with different thicknesses. As shown in Figs. 2C-D, the measured thickness of the BP nanosheet was in the range of 30-40 nm. Considering the random distribution of the thickness of BP made from the 'Scotch tape' method, the thickness of nanosheets in our sensor may vary from 10 to 60 nm. The thickness suggests the BP nanosheets have multiple layers. The Raman scattering measurement on the BP nanosheets is shown in Fig. 2B. Three Raman peaks located at around 359, 434 and 461 cm^{-1} are identified in the spectrum, which correspond with A_g^1, B_2g and A_g^2 modes of the pristine BP nanosheets, respectively. The Raman spectrum of the sample is in good agreement with previous observations (Buscema et al. 2014) (Liu et al. 2014).

To investigate the electrical characteristics of the BP FET device, at first, we performed an I-V measurement on the device. As shown in Fig. 3A, the typical resistance of BP devices ranges from 10^3 to 10^4 Ω, which depends on the density and thickness of the BP nanosheets on the electrodes. The device I-V curve shows a basically linear characteristic with slight bent, which indicates a small barrier at the interface between BP and the gold electrode. A Schottky barrier at the interface between the electrodes and the 2D nanomaterial can suppress charge transport (Popov et al. 2012). The small barrier height between BP and the gold electrode could degrade the performance since it lowers the charge injection efficiency from the electrode into BP. The BP nanosheet has a direct band gap that varies from 0.3 eV for the bulk BP to 2.0 eV for

the monolayer BP (Dai and Zeng 2014). The band gap of BP is thickness-dependent if the thickness is below 10 nm, while it becomes invariant for thicknesses above 10 nm (Li et al. 2014). Thick BP nanosheets (> 10 nm) can be assumed to have the same band gap, Fermi level, and thus the same carrier density (Cai et al. 2014). Therefore, the thick BP nanosheets (> 10 nm) have the same conductivity considering they also have the same carrier effective mass and mobility (Cai et al. 2014). The transistor measurement was carried out to study the semiconductor nature and the on-off current ratio of the BP device. The FET transfer curve of the BP device was characterized in air, in which a fixed bias (0.01 V) was applied across the channel and the gate voltage was swept from –40 to 40 V. The results show that BP is a typical p-type semiconductor by nature, with an on-off current ratio of 4 (Fig. 3B). Due to the scattering effect from the surface absorbed gas molecules, the as measured on-off ratio is smaller than the values measured in vacuum (Island et al. 2015). The electrical properties of the FET devices suggest that BP nanosheets could work as the channel material for high performance biosensors.

The sensing mechanism of the FET biosensor is based on the specific binding of the immobilized antibody probe and the antigen (Mao et al. 2011) (Song et al. 2010). The gate potential that is induced by the specific binding contributes to the change in carrier concentration/electrical conductivity of the sensing channel (Liu et al. 2012; Zhan et al. 2014). To study the BP FET sensor performance for IgG detection, at first, we characterized the dynamic response of the sensor to IgG with various concentrations. For the sensor test, 0.01× PBS buffer was pipetted onto the device first to create the baseline. The electrical conductivity of the sensor had an observable increase because the testing environment was switched from air to aqueous condition. After the signal became stable, antigens (IgG) with different concentrations (10-500 ng/mL, 1 μL) were then pipetted onto the anti-IgG immobilized device and the

conductivity of the BP increased correspondingly. The response (I_d) was recorded by a semiconductor analyzer with a constant bias (0.01 V) across the electrodes. Fig. 4A shows the dynamic response of a BP device with antibody probes. To quantitatively study the sensor response, the sensitivity is defined as $\Delta G/G_0$, where ΔG is the change of the device's electrical conductivity and G_0 is the original conductivity before the antigen injection. Since the source-drain voltage (V_{ds}) was fixed at 0.01 V, sensitivity can also be represented by $\Delta I/I_0$, where ΔI is the change in the source-drain current and I_0 is the baseline current. The sensitivity of the BP device increased from 5% to 10% when the concentration of IgG increased from 10 to 500 ng/ml. As shown in Fig. 4A, the sensor responds to the target protein instantaneously with a typical response time on the order of seconds.

Control experiments were carried out to better understand the role of gold NP-antibody conjugates. A BP device without anti-IgG probes was tested as a control group with exactly the same testing procedures. As shown in Fig. 4B, the sensor without probes showed slightly increased current responses to the IgG addition. However, the device current increases were unstable and the current gradually recovered to the original value after about 20-25 seconds. This phenomenon indicates that the slight response of the sensor may result from the non-specific binding of IgG molecules to the BP surface. Another control experiment was designed to study the selectivity of the BP device, in which a non-specific protein (avidin) was used as the antigen. As shown in Fig. 4C, after avidin was pipetted onto the BP biosensor with anti-IgG probes, a similar response as that of the device without probes was observed, indicating the nonspecific binding of proteins onto the BP surface will lead to fleeting signals. Fig. 4A shows a slightly different response to the PBS addition with Fig. 4B and C. This phenomenon can be ascribed to the mechanical perturbation upon drop casting the sample and the slightly loose

contact between BP and the electrode. The control experiments indicate that successful conjugation of antibody probes is critical for the specificity of the biosensor and the BP FET device is highly specific to a particular protein. Figure 4D plots the sensor sensitivity as a function of antigen concentration for normal devices with specific proteins, devices without probes, and devices with non-specific proteins. The anti-IgG immobilized devices show much higher sensitivities compared with the other two control groups. For non-specific binding groups, the sensitivity was negligible, although the concentration of IgG increased from 10 ng/ml to 500 ng/ml. IgG molecules carry negative surface charges in the PBS buffer (Lee et al. 2011). The probes specifically pick up the IgG molecules in the sample. The captured IgG molecules will induce a negative gate potential on the BP nanosheet and thus increase the drain-source current based on the p-type semiconducting nature of BP (Wang et al. 2014). Meanwhile, the charge transfer, which was supposed to decrease the drain-source current in this case, is minimized by the Al_2O_3 dielectric layer (Chang et al. 2013a). So the net effect of IgG adsorption onto the device is dominated by the gating effect, which is confirmed by the increased current in Fig. 4A. Fig. 4D also confirms that the BP FET biosensor has high selectivity towards a specific protein since the sensitivity for IgG is much higher than that for avidin.

The BP-based FET biosensor shares similar working principles with previously reported semiconducting 2D materials such as reduced graphene oxide (rGO) and MoS_2. For example, Mao et al. reported that the vertically-oriented graphene based FET sensor can detect IgG with a limit down to 2 ng/ml (Mao et al. 2013). There are also reports on using mechanically exfoliated graphene for protein detection with real-time response features (Ohno et al. 2010; Ohno et al. 2009). Table S1 in the Supporting Information shows a comparison of the sensing performance for BP, rGO and other 2D materials on protein detection. Compared with rGO and MoS_2, BP has

a finite band gap and a much higher carrier mobility, leading to an enhanced sensitivity (Cui et al. 2015). The BP FET biosensor has potential applications such as rapid diagnostics of diseases by detecting specific biomarker molecules and early screening of pestilence. The BP sensor's performance is dependent on the thickness of the nanosheet (Cui et al. 2015). If the distance between the probe and the channel is above the Debye length of the PBS buffer, the gating potential is completely screened considering that the conductance of channel is dominated by the BP layers adjacent to the electrode. Future work will be focused on further improving the performance of BP FET biosensors by controlling the thickness of the nanosheets and the antibody probe density.

4. Conclusions

In summary, we have demonstrated the outstanding performance of BP-based FET biosensors for protein detection. The as-produced BP device can detect IgG with a lower detection limit down to 10 ng/ml and a response time on the order of seconds. The surface of BP nanosheet was passivated by an Al_2O_3 dielectric layer for protecting BP from being oxidized in aqueous solutions. Thus, the electrical properties of BP can be preserved, leading to enhanced stability and sensitivity. Anti-IgG probes can be immobilized on the device through surface modifications of gold NPs and by doing so, IgG molecules specifically bind to antibody probes, thereby leading to the increase on the drain-source current due to the negative gate potential induced by the absorbed IgG. The major sensing mechanism for the surface passivated BP biosensor is the gating effect, instead of charge transfer, which is minimized by the Al_2O_3 passivation layer. The BP FET biosensor can potentially be used for precise and rapid diagnostics of diseases in point-of-care applications.

FIGURES

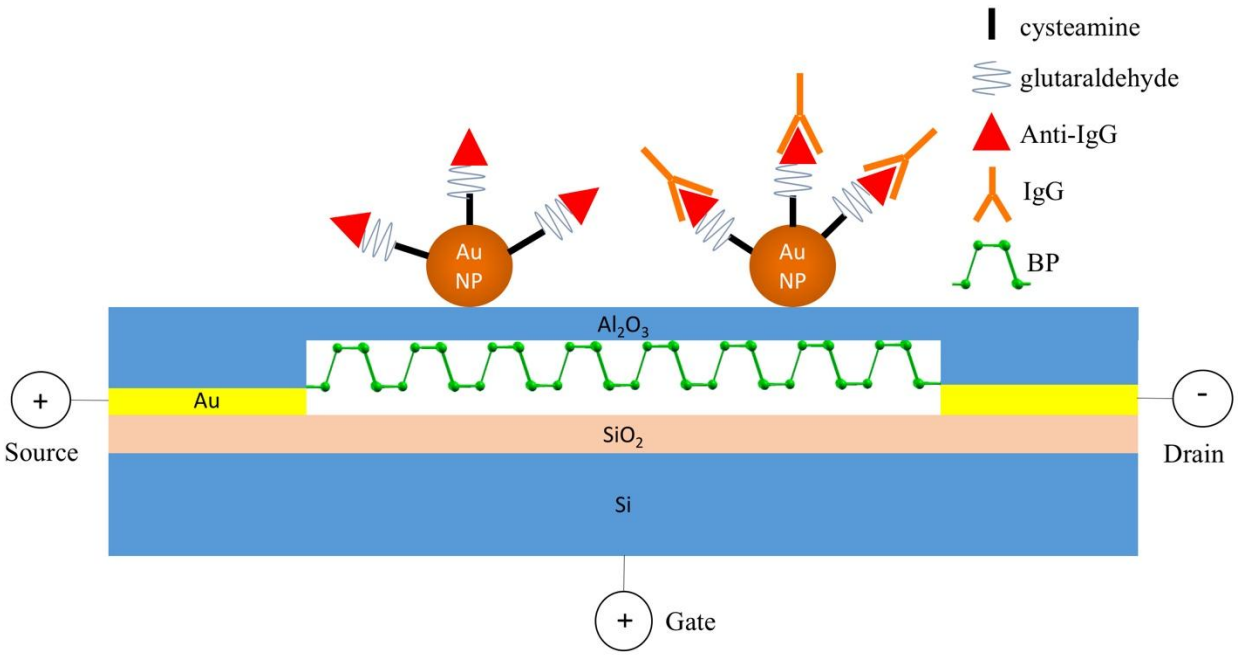

Figure 1. Schematic of the BP FET sensor. BP nanosheets were mechanically exfoliated and transferred onto the device, bridging the drain and source electrodes. Antibody probes were conjugated with Au NPs through chemical modifications. The Al_2O_3 dielectric layer was used to passivate the surface of BP nanosheet from being oxidized.

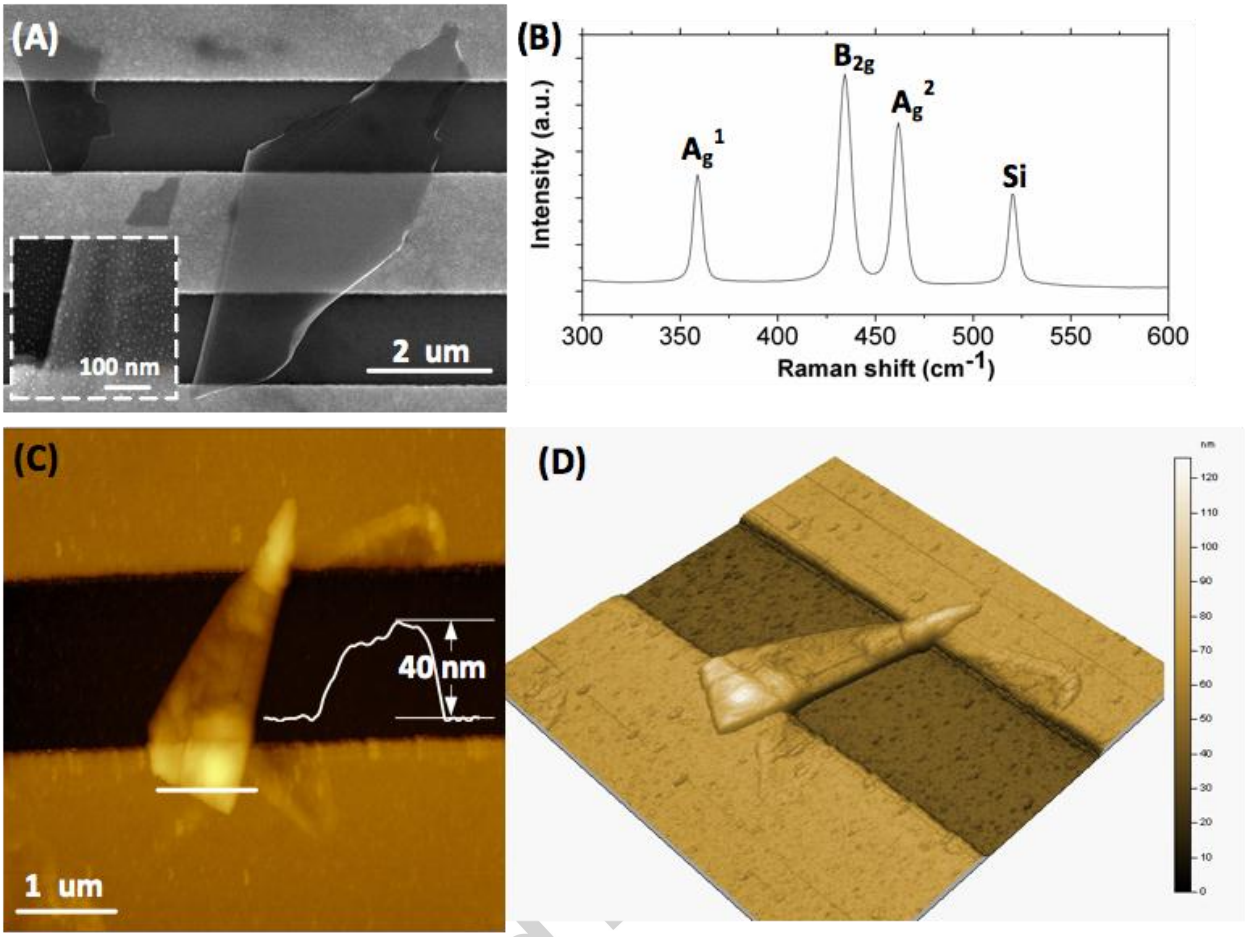

Figure 2. BP FET sensor characterization. (A) SEM image of mechanically exfoliated BP nanosheets on interdigitated gold electrodes. The inset shows the high magnification image of the BP nanosheet. Isolated and densely distributed gold NPs were observed on the surface of the BP nanosheet. (B) Raman spectrum of BP nanosheets. Three Raman peaks located at around 359, 434 and 461 cm^{-1} are identified in the spectrum. The 519 cm^{-1} peak is from the Si substrate. (C-D) AFM images of the BP nanosheet. (C) The thickness of the nanosheet was measured as 30 nm to 40 nm. (D) 3D view of the BP nanosheet positioned across the gold electrodes.

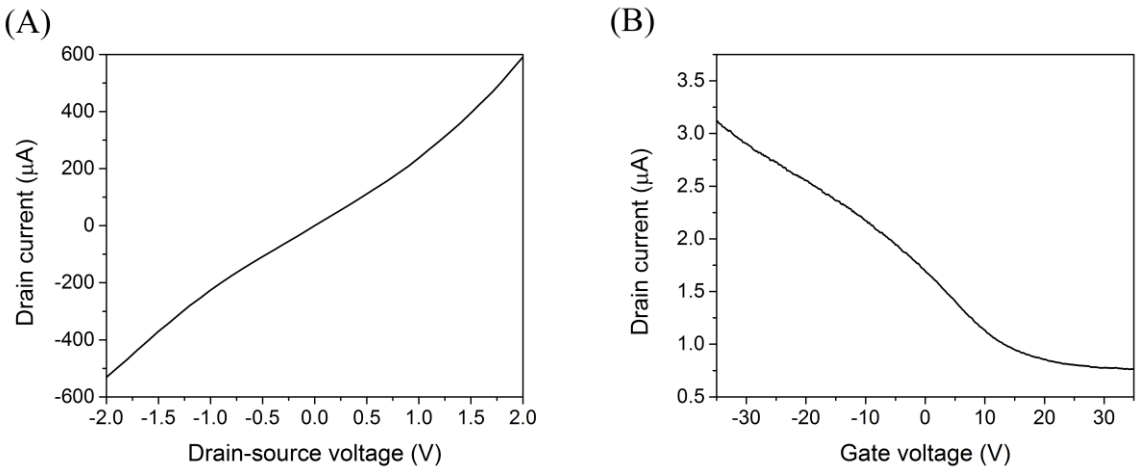

Figure 3. I-V and FET measurements on a typical sensor device. (A) Direct current measurement of the BP FET sensor, with the sensing channel labeled with gold NP-antibody conjugates. (B) Transistor measurement of the BP FET sensor. The drain-source voltage was fixed at 0.01 V.

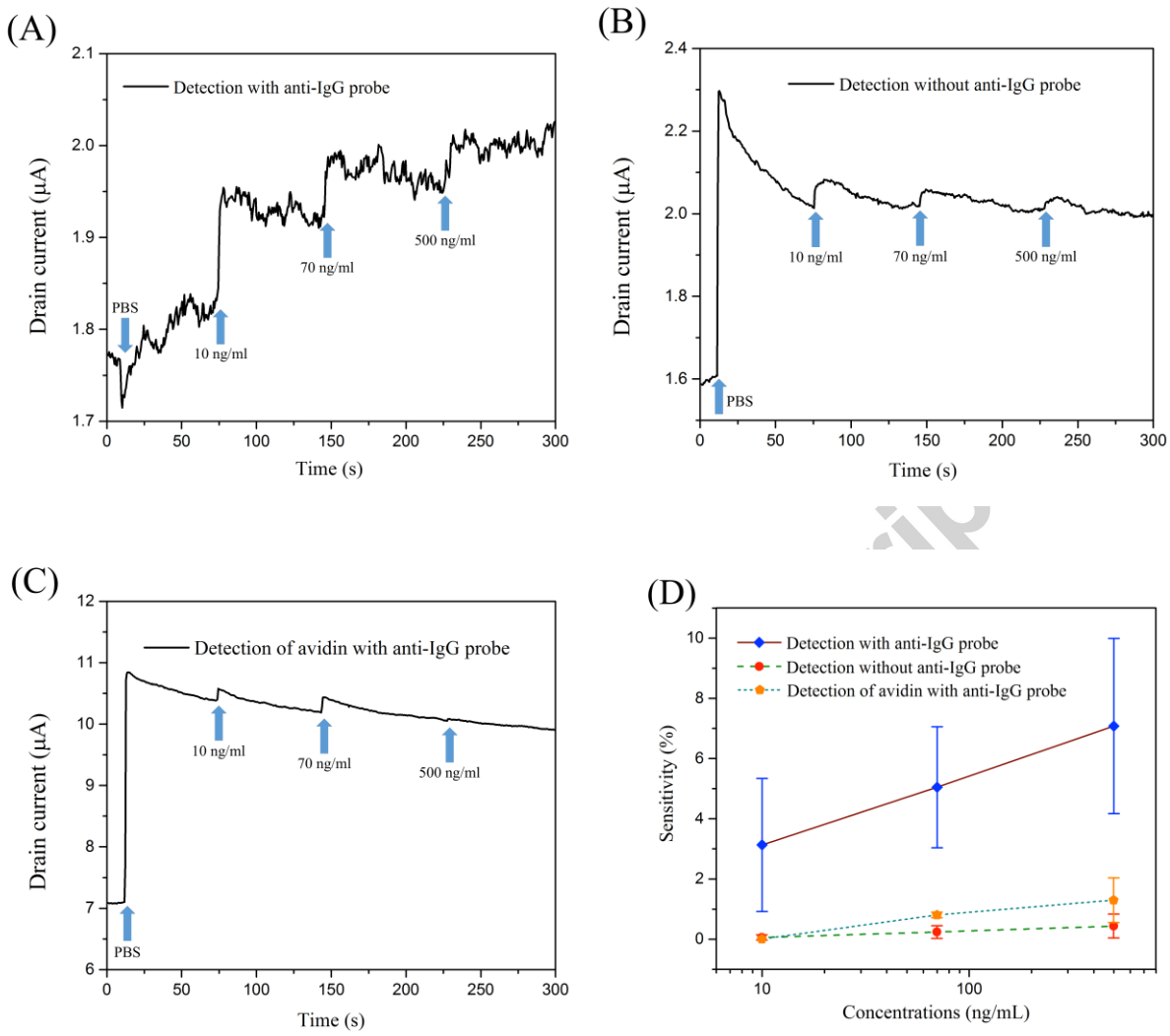

Figure 4. IgG detection with BP FET biosensors. (A) Dynamic response of the sensor for different concentrations of IgG. (B) Control experiment of non-specific binding to the BP sensor without antibody probes. (C) Control experiment of detecting a non-specific protein, i.e., avidin. For (A-C), the source-drain voltage was fixed at 0.01 V during the test. (D) Plotting of sensitivity as a function of target protein concentration. Specific binding of IgG molecules on the device leads to the highest sensitivity compared with the devices without probes and with non-specific proteins.

Acknowledgements

Financial support for this work was provided by the US National Science Foundation (IIP-1516207). The authors thank Dr. H. A. Owen for technical support with SEM analyses, and Dr. S. E. Hardcastle for technical support with AFM and Raman analyses. The SEM imaging was conducted at the Electron Microscope Laboratory of UWM. The AFM and Raman were conducted at the Advanced Analysis Facility of UWM.

Appendix A. Supplementary material

Supplementary data associated with this article can be found in the online version at:

Reference

Abbas, A.N., Liu, B., Chen, L., Ma, Y., Cong, S., Aroonyadet, N., Koepf, M., Nilges, T., Zhou, C., 2015. Black Phosphorus Gas Sensors. Acs Nano 9(5), 5618-5624.

Brent, J.R., Savjani, N., Lewis, E.A., Haigh, S.J., Lewis, D.J., O'Brien, P., 2014. Production of few-layer phosphorene by liquid exfoliation of black phosphorus. Chemical Communications 50(87), 13338-13341.

Buscema, M., Groenendijk, D.J., Blanter, S.I., Steele, G.A., van der Zant, H.S.J., Castellanos-Gomez, A., 2014. Fast and Broadband Photoresponse of Few-Layer Black Phosphorus Field-Effect Transistors. Nano Letters 14(6), 3347-3352.

Cai, Y., Zhang, G., Zhang, Y.W., 2014. Layer-dependent band alignment and work function of few-layer phosphorene. Sci Rep 4, 6677.

Chang, J., Mao, S., Zhang, Y., Cui, S., Steeber, D.A., Chen, J., 2013a. Single-walled carbon nanotube field-effect transistors with graphene oxide passivation for fast, sensitive, and selective protein detection. Biosensors & Bioelectronics 42, 186-192.

Chang, J., Zhou, G., Gao, X., Mao, S., Cui, S., Ocola, L.E., Yuan, C., Chen, J., 2015. Real-time detection of mercury ions in water using a reduced graphene oxide/DNA field-effect transistor with assistance of a passivation layer. Journal Name: Sensing and Bio-Sensing Research; Journal Volume: 5; Journal Issue: C, Medium: X; Size: p. 97-104.

Chang, J.B., Mao, S., Zhang, Y., Cui, S.M., Zhou, G.H., Wu, X.G., Yang, C.H., Chen, J.H., 2013b. Ultrasonic-assisted self-assembly of monolayer graphene oxide for rapid detection of Escherichia coli bacteria. Nanoscale 5(9), 3620-3626.

Chen, K.H., Lu, G.H., Chang, J.B., Mao, S., Yu, K.H., Cui, S.M., Chen, J.H., 2012. Hg(II) Ion Detection Using Thermally Reduced Graphene Oxide Decorated with Functionalized Gold Nanoparticles. Anal ChemAnal Chem 84(9), 4057-4062.

Coleman, J.N., Lotya, M., O'Neill, A., Bergin, S.D., King, P.J., Khan, U., Young, K., Gaucher, A., De, S., Smith, R.J., Shvets, I.V., Arora, S.K., Stanton, G., Kim, H.Y., Lee, K., Kim, G.T., Duesberg, G.S., Hallam, T., Boland, J.J., Wang, J.J., Donegan, J.F., Grunlan, J.C., Moriarty, G.,

Shmeliov, A., Nicholls, R.J., Perkins, J.M., Grieveson, E.M., Theuwissen, K., McComb, D.W., Nellist, P.D., Nicolosi, V., 2011. Two-Dimensional Nanosheets Produced by Liquid Exfoliation of Layered Materials. Science 331(6017), 568-571.
Cui, S., Pu, H., Wells, S.A., Wen, Z., Mao, S., Chang, J., Hersam, M.C., Chen, J., 2015. Ultrahigh sensitivity and layer-dependent sensing performance of phosphorene-based gas sensors. Nature communications 6.
Dai, J., Zeng, X.C., 2014. Bilayer Phosphorene: Effect of Stacking Order on Bandgap and Its Potential Applications in Thin-Film Solar Cells. J Phys Chem LettJ Phys Chem Lett 5(7), 1289-1293.
Island, J.O., Steele, G.A., van der Zant, H.S.J., Castellanos-Gomez, A., 2015. Environmental instability of few-layer black phosphorus. 2d Materials 2(1).
Koenig, S.P., Doganov, R.A., Schmidt, H., Castro Neto, A.H., Oezyilmaz, B., 2014. Electric field effect in ultrathin black phosphorus. Applied Physics Letters 104(10).
Late, D.J., Huang, Y.K., Liu, B., Acharya, J., Shirodkar, S.N., Luo, J.J., Yan, A.M., Charles, D., Waghmare, U.V., Dravid, V.P., Rao, C.N.R., 2013. Sensing Behavior of Atomically Thin-Layered MoS2 Transistors. Acs Nano 7(6), 4879-4891.
Lee, I., Luo, X., Cui, X.T., Yun, M., 2011. Highly sensitive single polyaniline nanowire biosensor for the detection of immunoglobulin G and myoglobin. Biosensors & Bioelectronics 26(7), 3297-3302.
Li, C., Curreli, M., Lin, H., Lei, B., Ishikawa, F.N., Datar, R., Cote, R.J., Thompson, M.E., Zhou, C.W., 2005. Complementary detection of prostate-specific antigen using ln(2)O(3) nanowires and carbon nanotubes. Journal of the American Chemical Society 127(36), 12484-12485.
Li, H., Yin, Z.Y., He, Q.Y., Li, H., Huang, X., Lu, G., Fam, D.W.H., Tok, A.I.Y., Zhang, Q., Zhang, H., 2012. Fabrication of Single- and Multilayer MoS2 Film-Based Field-Effect Transistors for Sensing NO at Room Temperature. Small 8(1), 63-67.
Li, L., Yu, Y., Ye, G.J., Ge, Q., Ou, X., Wu, H., Feng, D., Chen, X.H., Zhang, Y., 2014. Black phosphorus field-effect transistors. Nature Nanotechnology 9(5), 372-377.
Liu, H., Neal, A.T., Zhu, Z., Luo, Z., Xu, X.F., Tomanek, D., Ye, P.D.D., 2014. Phosphorene: An Unexplored 2D Semiconductor with a High Hole Mobility. Acs Nano 8(4), 4033-4041.
Liu, Y., Dong, X., Chen, P., 2012. Biological and chemical sensors based on graphene materials. Chemical Society Reviews 41(6), 2283-2307.
Mao, S., Lu, G., Yu, K., Bo, Z., Chen, J., 2010. Specific Protein Detection Using Thermally Reduced Graphene Oxide Sheet Decorated with Gold Nanoparticle-Antibody Conjugates. Advanced Materials 22(32), 3521-+.
Mao, S., Yu, K., Chang, J., Steeber, D.A., Ocola, L.E., Chen, J., 2013. Direct Growth of Vertically-oriented Graphene for Field-Effect Transistor Biosensor. Scientific Reports 3.
Mao, S., Yu, K., Lu, G., Chen, J., 2011. Highly Sensitive Protein Sensor Based on Thermally-Reduced Graphene Oxide Field-Effect Transistor. Nano Research 4(10), 921-930.
Ohno, Y., Maehashi, K., Matsumoto, K., 2010. Label-free biosensors based on aptamer-modified graphene field-effect transistors. J Am Chem Soc 132(51), 18012-18013.
Ohno, Y., Maehashi, K., Yamashiro, Y., Matsumoto, K., 2009. Electrolyte-gated graphene field-effect transistors for detecting pH and protein adsorption. Nano Lett 9(9), 3318-3322.
Popov, I., Seifert, G., Tomanek, D., 2012. Designing Electrical Contacts to MoS2 Monolayers: A Computational Study. Physical Review Letters 108(15).
Radisavljevic, B., Kis, A., 2013. Measurement of mobility in dual-gated MoS2 transistors. Nature Nanotechnology 8(3), 147-148.

Radisavljevic, B., Radenovic, A., Brivio, J., Giacometti, V., Kis, A., 2011. Single-layer MoS2 transistors. Nature Nanotechnology 6(3), 147-150.
Sarkar, D., Liu, W., Xie, X.J., Anselmo, A.C., Mitragotri, S., Banerjee, K., 2014. MoS2 Field-Effect Transistor for Next-Generation Label-Free Biosensors. Acs Nano 8(4), 3992-4003.
Schedin, F., Geim, A.K., Morozov, S.V., Hill, E.W., Blake, P., Katsnelson, M.I., Novoselov, K.S., 2007. Detection of individual gas molecules adsorbed on graphene. Nature Materials 6(9), 652-655.
Song, S., Qin, Y., He, Y., Huang, Q., Fan, C., Chen, H.-Y., 2010. Functional nanoprobes for ultrasensitive detection of biomolecules. Chemical Society Reviews 39(11), 4234-4243.
Wang, L., Wang, Y., Wong, J.I., Palacios, T., Kong, J., Yang, H.Y., 2014. Functionalized MoS2 Nanosheet-Based Field-Effect Biosensor for Label-Free Sensitive Detection of Cancer Marker Proteins in Solution. Small 10(6), 1101-1105.
Wood, J.D., Wells, S.A., Jariwala, D., Chen, K.-S., Cho, E., Sangwan, V.K., Liu, X., Lauhon, L.J., Marks, T.J., Hersam, M.C., 2014. Effective Passivation of Exfoliated Black Phosphorus Transistors against Ambient Degradation. Nano Letters 14(12), 6964-6970.
Xia, F., Wang, H., Jia, Y., 2014. Rediscovering black phosphorus as an anisotropic layered material for optoelectronics and electronics. Nature Communications 5.
Yang, K., Zhang, S.A., Zhang, G.X., Sun, X.M., Lee, S.T., Liu, Z.A., 2010. Graphene in Mice: Ultrahigh In Vivo Tumor Uptake and Efficient Photothermal Therapy. Nano Letters 10(9), 3318-3323.
Zhan, B., Li, C., Yang, J., Jenkins, G., Huang, W., Dong, X., 2014. Graphene Field-Effect Transistor and Its Application for Electronic Sensing. Small 10(20), 4042-4065.
Zhang, W., Tien, H., Xiu, P., Zhou, B., Ye, C., Luan, B., Zhou, R., 2015. Revealing the importance of surface morphology of nanomaterials to biological responses: Adsorption of the villin headpiece onto graphene and phosphorene. Carbon 94, 895-902.

Field-Effect Transistor Biosensors with Two-dimensional Black Phosphorus Nanosheets

Yantao Chen [a], Ren Ren [a], Haihui Pu [a], Jingbo Chang [a], Shun Mao [a,b,], Junhong Chen [a,]**

[a] Department of Mechanical Engineering, University of Wisconsin-Milwaukee, 3200 N. Cramer Street, Milwaukee, WI 53211, USA

[b] State Key Laboratory of Pollution Control and Resource Reuse, School of Environmental Science and Engineering, Tongji University, 1239 Siping Road, Shanghai 200092, PR China

*Corresponding authors. E-mail addresses: jhchen@uwm.edu (J. Chen), shunmao@uwm.edu (S. Mao)

TOC

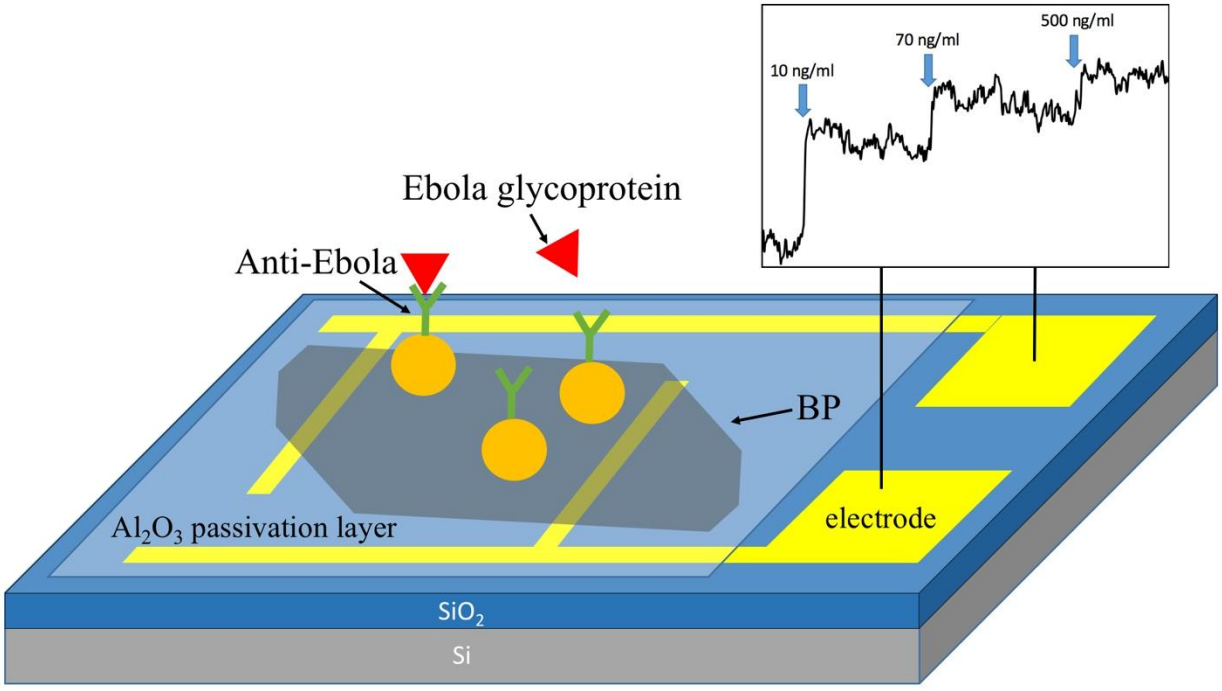

Highlights

- A black phosphorous (BP) nanosheet field-effect transistor biosensor is reported.
- A surface passivation layer is used to enable stable operation of the BP biosensor.
- The biosensor shows fast response, high sensitivity, and selectivity for IgG protein.
- The sensing mechanism is dominated by the gating effect instead of charge transfer.